Quantization for lattice-gas models of water

David R. Herrick* and Frank H. Stillinger

Bell Laboratories, Murray Hill, New Jersey 07974
(Received 12 March 1976)

Several recent studies have shown that some of the unusual properties of liquid water can be reproduced with a classical lattice-gas model, wherein the host lattice is body-centered cubic. In this paper we quantize both rotational and translational motion in those models, using suitable hopping operators. Several alternative forms are possible for the rotational kinetic energy; we provide comparisons for each with the experimental spectrum. Variational calculations have been performed for $(H_2O)_2$, $(D_2O)_2$, and $(T_2O)_2$ ground states on the lattice to estimate hydrogen bond destabilization by zero-point motion. Finally, expressions have been developed for thermodynamic-property and distribution-function quantum corrections that should be useful in classical lattice-gas simulations of water via computer.

I. INTRODUCTION

Several versions of a lattice-gas model for water have recently been studied[1-4] in order to understand the molecular ordering and thermodynamic properties of that liquid. Each of these versions has relied exclusively on classical statistical mechanics in spite of the fact that substantial quantum effects should be present for molecules with inertial moments as small as those in water. It is the goal of the present paper to introduce quantization into lattice-gas models for water, and to draw some useful conclusions therefrom.

Conventionally, the statistical mechanics of classical lattice gases concentrates attention on the configurational counting problem. Particle kinetic energy is fully separated in this limit, and need not be considered. However, the quantum corrections to the classical limit arise largely from noncommutivity of kinetic and potential energy operators, so both operators must be present and explicit from the outset if one is to calculate these corrections.

In the case of lattice gases consisting of structureless particles, a systematic procedure has been developed for generating quantum corrections to the conventional classical limit.[5] In that case the kinetic energy operator for each particle consisted of a hopping operator capable of moving that particle from site to site by nearest-neighbor shifts. The present circumstance requires discrete hops both in position *and* orientation.

The simplest lattice on which water can realistically be modelled is the body-centered cubic lattice.[2-4] The oxygen atom of each molecule resides at (or very near to) a site, and its covalent OH bonds are permitted to point toward pairs of nearest-neighbor sites which sit across a cube face from one another. Figure 1 illustrates this geometry. It is possible to construct a cubic ice crystal on this lattice, using half of the sites, with each molecule hydrogen bonded to four nearest neighbors in a tetrahedral pattern. Nominally, the HOH bond angle for water molecules fitted to this lattice would be the tetrahedral angle 109.47°, only slightly larger than the free molecule angle 104.5°.[6]

It is clear from Fig. 1 that each molecule is permitted 24 distinct orientations at any given lattice site. The melting of the cubic ice crystal presumably results from both rotational disorder and translational disorder, since either type of motion can separately disrupt the fully formed tetrahedral network of hydrogen bonds.

In the present context, we presume that the total kinetic energy operator $\mathbf{T}$ for N water molecules in the lattice has the following form:

$$\mathbf{T} = \sum_{i=1}^{N} (\mathbf{T}_{ti} + \mathbf{T}_{ri}). \tag{1.1}$$

Here $\mathbf{T}_{ti}$ stands for the translational kinetic energy for molecule i, and $\mathbf{T}_{ri}$ stands for its rotational kinetic energy. Acting on a function Ψ of position α_i and orientation ω_i for molecule i, the translational operator $\mathbf{T}_{ti}$ has the property[5]

$$\mathbf{T}_{ti}\Psi(\alpha_i, \omega_i) = \frac{\hbar^2}{2ml^2}\left[8\Psi(\alpha_i, \omega_i) - \sum_{\alpha_i'} \Psi(\alpha_i', \omega_i)\right] \tag{1.2}$$

(this is merely a discrete version of the conventional Laplacian), where m is the molecular mass, the sum spans the eight nearest-neighbor sites for α_i, and distance l is $2/\sqrt{3}$ times the nearest-neighbor spacing.

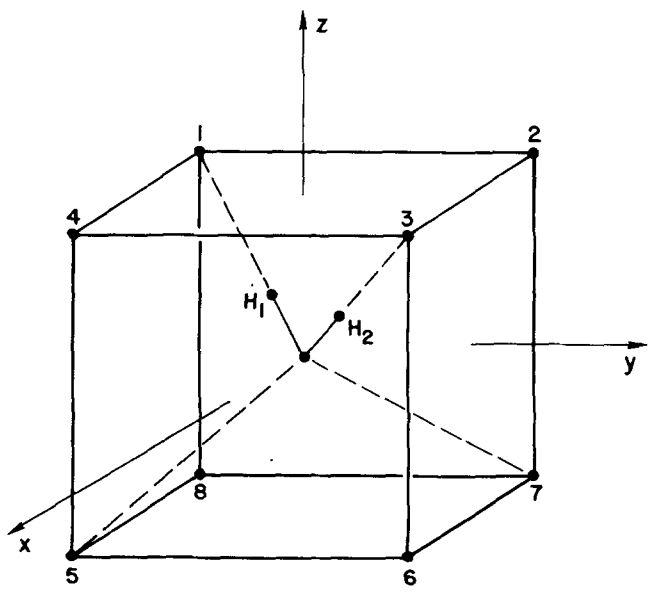

FIG. 1. The body-centered cubic lattice of water.

The following section introduces specific forms for the rotational kinetic energy operators $\mathbf{T}_{ri}$. The corresponding rotational spectra of single-molecule eigenstates are then deduced and compared to experiment.

Section III contains an examination of the potential energy functions that are appropriate for lattice-gas models of water. In particular, we display there a nearest-neighbor version for an additive pair potential that seems adequate to induce local order of the type thought to be present in liquid water.

A variational study of binding in the water dimer appears in Sec. IV.

High-temperature quantum corrections for lattice-gas water (including both thermodynamic properties and distribution functions) are stated and discussed in Sec. V. Although it is difficult to evaluate these corrections under condensed-phase conditions, we anticipate that the formulas exhibited will find important application in connection with computer simulation studies.

II. ROTATIONAL LATTICE SPECTRUM OF WATER

A. Lattice states

The 24 rotational states ω for a water molecule on a given lattice site may temporarily be denoted by $|jk\rangle$, where the indices j and k identify neighbor sites toward which OH groups point (see Fig. 1). Elementary rotations consist of transitions between these 24 states. The rotational energy operator must be invariant with respect to the rotation–inversion–permutation symmetry group for the H_2O molecule. In the present case of a cubic rotation lattice, the 24 proper rotations form the octahedral point group O. For a complete description of this group and the related notation we refer the reader to one of the standard texts.[7] In particular, the representation Γ of lattice states is regular in O, with

$$\Gamma = A_1 + A_2 + 2E + 3T_1 + 3T_2. \tag{2.1}$$

Further classification with respect to inversion i and hydrogen exchange P_{12} (e.g., $i|13\rangle = |68\rangle$, $P_{12}|13\rangle = |31\rangle$) yields the following irreducible representations:

$$\Gamma = A_{1g}^{+} + A_{2u}^{+} + E_u^{+} + E_g^{+} + T_{1u}^{+} + T_{2g}^{+} + T_{1u}^{-} + T_{1g}^{-} + T_{2g}^{-} + T_{2u}^{-}. \tag{2.2}$$

Here (g/u) indicates (even/odd) character with respect to inversion, and $(+/-)$ labels (even/odd) exchange symmetry. Exchange symmetrized elementary states are

$$s_{jk} = (|jk\rangle + |kj\rangle)/\sqrt{2}, \qquad a_{jk} = (|jk\rangle - |kj\rangle)/\sqrt{2}, \tag{2.3}$$

with

$$(P_{12} - 1)s_{jk} = (P_{12} + 1)a_{jk} = 0.$$

Basis functions for the irreducible representations in Eq. (2.2) were constructed using standard group theoretical projection operator techniques. These lattice rotation states appear in Tables I and II for even and odd exchange parity, respectively. The multidimensional representations E_g, T_1, and T_2 have been labelled in terms of their transformation properties with respect to the x, y, and z axes of Fig. 1. The basis is orthonormal for the inner product,

$$\langle jk | lm \rangle = \delta_{jl}\delta_{km}. \tag{2.4}$$

Since each irreducible representation in Eq. (2.2) appears only once, the group theoretical lattice states diagonalize the (as yet unspecified) rotational hopping Hamiltonian for water, giving a total of 10 distinct energy levels. We thus find ourselves in the position of knowing the eigenfunctions of the Hamiltonian independently of its precise form, subject only to its invariance with respect to the product group of space-fixed lattice rotations, inversions, and exchange.

B. General form of the hopping Hamiltonian

Since the water molecule is an asymmetric rotor, the lattice rotation energy cannot be expressed solely in terms of the five classes of equivalent rotations for the

TABLE I. Group theoretically constructed lattice rotation states having even exchange symmetry.

		Mixing coefficients of elementary states[a]												
	State	S_{13}	S_{68}	S_{24}	S_{57}	S_{15}	S_{26}	S_{48}	S_{37}	S_{17}	S_{46}	S_{35}	S_{28}	N
1.	A_{1g}^{+}	1	1	1	1	1	1	1	1	1	1	1	1	12
2.	$T_{1u}^{+}(z)$	1	−1	1	−1	0	0	0	0	0	0	0	0	4
3.	$T_{1u}^{+}(x)$	0	0	0	0	0	0	0	0	−1	1	1	−1	4
4.	$T_{1u}^{+}(y)$	0	0	0	0	−1	1	−1	1	0	0	0	0	4
5.	$E_g^{+}(3z^2-r^2)$	2	2	2	2	−1	−1	−1	−1	−1	−1	−1	−1	24
6.	$E_g^{+}(x^2-y^2)$	0	0	0	0	−1	−1	−1	−1	1	1	1	1	8
7.	E_u^{+}	0	0	0	0	1	−1	−1	1	−1	1	−1	1	8
8.	E_u^{+}	2	−2	−2	2	−1	1	1	−1	−1	1	−1	1	24
9.	$T_{2g}^{+}(xy)$	1	1	−1	−1	0	0	0	0	0	0	0	0	4
10.	$T_{2g}^{+}(yz)$	0	0	0	0	0	0	0	0	−1	−1	1	1	4
11.	$T_{2g}^{+}(zx)$	0	0	0	0	−1	−1	1	1	0	0	0	0	4
12.	A_{2u}^{+}	1	−1	−1	1	1	−1	−1	1	1	−1	1	−1	12

[a] $\phi = N^{-1/2}\sum S_{jk}C_{jk}$, where the C_{jk} are tabulated here.

TABLE II. Group theoretically constructed lattice rotation states having odd exchange symmetry.

State		Mixing coefficients of elementary states[a]												
		a_{13}	a_{68}	a_{24}	a_{57}	a_{15}	a_{26}	a_{48}	a_{37}	a_{17}	a_{46}	a_{35}	a_{28}	N
1.	$T^-_{1u}(z)$	0	0	0	0	−1	−1	−1	−1	−1	−1	−1	−1	8
2.	$T^-_{1u}(y)$	1	−1	−1	1	0	0	0	0	1	1	−1	−1	8
3.	$T^-_{1u}(x)$	1	−1	1	−1	1	1	−1	−1	0	0	0	0	8
4.	$T^-_{1g}(R_z)$	0	0	0	0	1	−1	−1	1	−1	1	−1	1	8
5.	$T^-_{1g}(R_y)$	1	1	1	1	0	0	0	0	−1	1	1	−1	8
6.	$T^-_{1g}(R_x)$	−1	−1	1	1	1	−1	1	−1	0	0	0	0	8
7.	$T^-_{2g}(xy)$	0	0	0	0	−1	1	1	−1	−1	1	−1	1	8
8.	$T^-_{2g}(zx)$	1	1	1	1	0	0	0	0	1	−1	−1	1	8
9.	$T^-_{2g}(yz)$	1	1	−1	−1	1	−1	1	−1	0	0	0	0	8
10.	$T^-_{2u}(z_y{}^2-zx^2)$	0	0	0	0	−1	−1	−1	−1	1	1	1	1	8
11.	$T^-_{2u}(yz^2-yx^2)$	1	−1	−1	1	0	0	0	0	−1	−1	1	1	8
12.	$T^-_{2u}(xz^2-xy^2)$	1	−1	1	−1	−1	−1	1	1	0	0	0	0	8

[a] $\phi = N^{-1/2}\sum a_{jk}d_{jk}$, where the d_{jk} are tabulated here.

octahedral group: $1E$, $6C_4$, $8C_3$, $3(C_2 = C_4^2)$, and $6C_2$. Instead we must classify the types of possible rotations with respect to a body-fixed set of axes. We therefore adopt the convention here that the x, y, and z axes in Fig. 1 represent a body-fixed system for the configuration $|13\rangle$. Principal axes for the molecule are then $a = (x+y)/\sqrt{2}$, $b = z$, and $c = (x-y)/\sqrt{2}$. There are 10 distinct types of rotations for this internal reference frame, consisting of subdivisions of the six octahedral rotation classes. They are the identity operator E, plus

$$6C_4 = 2C_4^b + 4C_4^\perp, \quad 8C_3 = 4C_3^{\parallel} + 4C_3^\perp,$$
$$3C_2 = C_2^b + 2C_2^\perp, \quad 6C_2 = C_2^a + C_2^c + 4C_2^e. \tag{2.5}$$

Here a, b, and c label the principal axes, and e labels axes bisecting the cube edges excluding a, b, and c. The label $\parallel$ denotes rotation axes within the plane of the molecule, while $\perp$ rotation axes have a nonvanishing component normal to the molecular plane. All rotations of a given type are equivalent, so that the lattice rotational Hamiltonian is characterized at most by 10 parameters. The totally symmetric A_{1g}^+ ground state can be assigned zero energy, thus reducing the number of independent parameters to nine.

The rotational kinetic energy can be written in the following general form:

$$T_r = \sum_{k=1}^{9} w_k t_k, \tag{2.6}$$

where the w_k are parameters and the t_k are a set of reduced energy operators for the distinct types of rotations. They are

$$t_1 = 2 - \sum C_4^b, \quad t_2 = 4 - \sum C_4^\perp, \quad t_3 = 4 - \sum C_3^{\parallel},$$
$$t_4 = 4 - \sum C_3^\perp, \quad t_5 = 1 - C_2^b, \quad t_6 = 2 - \sum C_2^\perp, \tag{2.7}$$
$$t_7 = 1 - C_2^a, \quad t_8 = 1 - C_2^c, \quad t_9 = 4 - \sum C_2^e,$$

where $\sum$ denotes a summation over all rotations of the type specified. For instance,

$$t_7|57\rangle = |57\rangle - |24\rangle \tag{2.8}$$

and

$$t_3|13\rangle = 4|13\rangle - |15\rangle - |17\rangle - |53\rangle - |73\rangle. \tag{2.9}$$

The t_k constitute a mutually commuting set of operators which are diagonal in the group theoretical basis, since the operators are invariant under all space-fixed lattice symmetry operations. In addition, it is possible to express all of the t_k in terms of the four operators t_1, t_2, i, and P_{12}. Specifically, this representation is

$$t_3 = 4 + (t_2 - 4)iP_{12}, \quad t_4 = 4 + (t_2 - 4)i,$$
$$t_5 = 1 - P_{12}, \quad t_6 = 2 + (t_1 - 2)i, \tag{2.10}$$
$$t_7 = 1 - iP_{12}, \quad t_8 = 1 - i,$$
$$t_9 = 4 + (t_2 - 4)P_{12}.$$

For use in subsequent sections we define also

$$D^2 = t_1 + t_2, \quad D_b^2 = t_1. \tag{2.11}$$

Note that $D^2 = 6 - \sum C_4$, where the summation covers the six C_4 rotations. Eigenvalues of D^2 are obtained easily using the theory of finite groups,[7] namely, if $\mathfrak{C}$ is a class of operations in a group G of order h, and if the operator $I_{\mathfrak{C}}$ is the sum over all group elements $R \in \mathfrak{C}$, then $I_{\mathfrak{C}}$ is diagonal on any basis φ_k of irreducible representations of G, with

$$I_{\mathfrak{C}}\varphi_k = (N_{\mathfrak{C}}\chi^k(\mathfrak{C})/l_k)\varphi_k. \tag{2.12}$$

Here l_k is the dimension of the kth irreducible representation, $\chi^k(\mathfrak{C})$ is the corresponding character under $\mathfrak{C}$, and $N_{\mathfrak{C}}$ is the number of elements in $\mathfrak{C}$.

This result has general applicability to the theory of rotational spectra of lattices. In our model it allows D^2, $t_3 + t_4$, $t_5 + t_6$, and $t_7 + t_8 + t_9$ to be evaluated simply, requiring only the use of the character table for the

TABLE III. Eigenvalues of the elementary rotation hopping kinetic energy operators t_k for the 10 lattice energy levels.

				Hopping operator							
	Level	D^2	$D_b^2=t_1$	t_2	t_3	t_4	t_5	t_6	t_7	t_8	t_9
1.	A_{1g}^+	0	0	0	0	0	0	0	0	0	0
2.	T_{1u}^-	4	2	2	2	6	2	2	0	2	6
3.	T_{1u}^+	4	0	4	4	4	0	4	2	2	4
4.	T_{1g}^-	4	2	2	6	2	2	2	2	0	6
5.	E_u^+	6	4	2	6	6	0	0	2	2	2
6.	E_g^+	6	0	6	6	6	0	0	0	0	6
7.	T_{2g}^-	8	2	6	2	6	2	2	2	0	2
8.	T_{2g}^+	8	4	4	4	4	0	4	0	0	4
9.	T_{2u}^-	8	2	6	6	2	2	2	0	2	2
10.	A_{2u}^+	12	4	8	0	0	0	0	2	2	8

octahedral group. A compilation of eigenvalues for the t_k appears in Table III.

Equation (2.6) permits empirical energy operators to be defined by fitting the coefficients w_k to give nine excited states of the H_2O rotational spectrum. This procedure is not unique, since there exists no unambiguous criterion for selecting the states for the fitting. In order eventually to estimate quantum corrections to thermodynamic properties of the lattice-gas model it may be advantageous to use a simpler form of T_r, involving only a few of the physically important t_k. Indeed, we feel that fits to the spectrum involving high energy levels is not justified due to the coarseness of the 24-state rotational lattice. We therefore pursue in Sec. II C the derivation of a simple nearest-neighbor hopping Hamiltonian which is sufficiently accurate for estimating at least the gross features of the rotational spectrum.

The operator T_r in Eq. (2.6) is applicable only to H_2O and its isotopes D_2O and T_2O. Mixed isotopes such as HOD destroy the exchange symmetry. However, due to the limited number of states in the cubic rotational lattice, exchange remains a good quantum number in all energy levels except T_{1u}^+ and T_{2g}^+. The form of the hopping Hamiltonian would have to be altered accordingly for mixed isotopes. In this initial investigation we consider only isotopic species having C_{2v} symmetry.

C. Derivation of an approximate single-molecule Hamiltonian

The energy levels of an asymmetric rotor (for which the full range of Euler angles is permitted) are eigenvalues of[8]

$$\mathbf{F}=A\mathbf{J}_a^2+B\mathbf{J}_b^2+C\mathbf{J}_c^2. \tag{2.13}$$

Here $\mathbf{J}_a$, $\mathbf{J}_b$, and $\mathbf{J}_c$ are the projections of the angular momentum operator J along the principal axes of the molecule. The rotational constants satisfy $A>B>C$, and for convenience the experimental constants of Bellet *et al.*[9] for water isotopes are displayed in Table IV. We seek a discretized version of F on the lattice, and expect that the spectrum of the hopping Hamiltonian will reproduce at most only the lower portion of the exact spectrum. This stems from the inherent deficiency of any lattice in attempting to represent the oscillatory structure of the energy wavefunctions.

The continuous operators $\mathbf{J}_x$ and $\mathbf{J}_x^2$ for angular momentum about an arbitrary axis x can be approximated with finite rotations through an angle α as follows:

$$\mathbf{J}_x\to[\exp(i\alpha\mathbf{J}_x)-\exp(-i\alpha\mathbf{J}_x)]/2i\alpha, \tag{2.14}$$

$$\mathbf{J}_x^2\to[2-\exp(i\alpha\mathbf{J}_x)-\exp(-i\alpha\mathbf{J}_x)]/\alpha^2. \tag{2.15}$$

These representations become exact in the limit $\alpha\to 0$, but may not always give accurate approximations for finite α. In this connection note that only C_2 rotations are possible about the a and c axes, requiring $|\alpha|$ to be no smaller than π (although C_4 rotations with $|\alpha|=\pi/2$ can occur about b). Using Eq. (2.15) to discretize F gives

$$\mathbf{F}\to(2/\pi)^2[\tfrac{1}{2}A(1-iP_{12})+BD_b^2+\tfrac{1}{2}C(1-i)], \tag{2.16}$$

which yields a spectrum bearing little resemblance to the exact asymmetric rotor energy levels. The first excited lattice state is the T_{1u}^- level having an energy $(2/\pi)^2(2B+C)=15.53\ \mathrm{cm}^{-1}$, which is significantly lower than the experimental[10] $J_\tau=1_{-1}$ level at $23.79\ \mathrm{cm}^{-1}$.

We expect that more accurate representations of F will result from discretizations in which the angle α assumes the smallest possible values for a given lattice, so as to describe only the nearest-neighbor rotational hops. These are C_4 rotations in the present model, defined about the x, y, and $z(=b)$ axes for the $|13\rangle$ orientation in Fig. 1. In order to utilize these rotations we rewrite F in the equivalent form

$$\mathbf{F}=\tfrac{1}{2}(A+C)(\mathbf{J}_x^2+\mathbf{J}_y^2+\mathbf{J}_b^2)+\tfrac{1}{2}(2B-A-C)\mathbf{J}_b^2 +\tfrac{1}{2}(A-C)(\mathbf{J}_x\mathbf{J}_y+\mathbf{J}_y\mathbf{J}_x), \tag{2.17}$$

where cross terms are to be represented as products of discretizations about perpendicular axes. Thus, for instance,

$$\mathbf{J}_x\mathbf{J}_y\to(C_4^{+x}-C_4^{-x})(C_4^{-y}-C_4^{+y})/\pi^2, \tag{2.18}$$

where C_4^{+x} and C_4^{-x} are $+90^\circ$ and -90° rotations, respectively, about the x axis. The discrete lattice representation of F is then

$$\mathbf{F}\to(2/\pi)^2[\tfrac{1}{2}(A+C)D^2+\tfrac{1}{2}(2B-A-C)D_b^2+\tfrac{1}{8}(A-C)(t_3-t_4)]. \tag{2.19}$$

The term t_3-t_4 involves C_3 rotations which result from products of two C_4 rotations. The lowest excited rotational for Eq. (2.19) is T_{1u}^- having an energy $(2/\pi)^2\times[\frac{1}{2}A+2B+\frac{3}{2}C]$, or $23.06\ \mathrm{cm}^{-1}$ for H_2O. Higher excited states tend to be substantially lower than the exact asymmetric rotor levels, but nevertheless they repre-

TABLE IV. Rotational constants for water isomers in cm^{-1}, adapted from Ref. 9.

	H_2O	D_2O	T_2O
A	27.88	15.42	11.30
B	14.52	7.27	4.86
C	9.28	4.85	3.30

TABLE V. Lattice rotational energies for the operators T_τ^0 and R^0.

State	Energy	
	T_τ^0	R^0
A_{1g}^+	0	0
T_{1u}^-	$B+C$	$\frac{2}{3}(A+B+C)$
T_{1u}^+	$A+C$	
T_{1g}^-	$A+B$	
E_u^+	$\frac{1}{2}(A+C)+2B$	$A+B+C$
E_g^+	$\frac{3}{2}(A+C)$	
T_{2g}^-	$A+B+2C$	$\frac{4}{3}(A+B+C)$
T_{2g}^+	$A+2B+C$	
T_{2u}^-	$2A+B+C$	
A_{2u}^+	$2(A+B+C)$	$2(A+B+C)$

sent a significant improvement over the spectrum of Eq. (2.16).

These results suggest a semiempirical Hamiltonian of the form

$$T_\tau^0=\beta_\tau[\tfrac{1}{2}(A+C)D^2+\tfrac{1}{2}(2B-A-C)D_b^2]+\gamma_\tau[\tfrac{1}{2}(A-C)(t_3-t_4)], \tag{2.20}$$

where β_τ and γ_τ are to be chosen to represent as well as possible the lower energy region of the spectrum. For $\beta_\tau=\frac{1}{2}$ and $\gamma_\tau=\frac{1}{4}$, T_τ^0 generates the three lowest excited asymmetric rotor levels[8] exactly, while retaining nearly the same spectrum for the higher states as that from Eq. (2.19). The energy levels of T_τ^0 appear in Table V as functions of A, B, and C. The spectrum consists of pairs of levels symmetrically displaced above and below an average energy $\overline{T}_\tau^0=A+B+C$.

T_τ^0 should be more than sufficient for estimating quantum corrections to thermodynamic properties of the lattice gas. In fact it may be advantageous instead to use the even simpler approximation $\mathbf{F}\sim R^0$, with

$$R^0=\tau D^2. \tag{2.21}$$

This form corresponds to representing water as a spherical rotor on the cubic orientation lattice. Normalization of the spectrum can be achieved by fitting τ so that the degenerate T_1 levels (cf Table III) are equal to the average energy of the exact $J=1$ level. This method gives

$$\tau=(A+B+C)/6, \tag{2.22}$$

and the resulting spectrum of R^0 appears in Table V with that of T_τ^0. Note that the average energy $\overline{R}^0=A+B+C=\overline{T}_\tau^0$.

D. Comparison with experimental spectrum

Clearly there does not exist a one-to-one correspondence of lattice rotation levels with the exact asymmetric rotor levels[8] J_τ. Instead, each lattice state represents a mixture of J_τ levels, with perhaps only several low-lying states contributing significantly to the mixture in some cases. We consider here transformation properties of the exact rotational states with respect to the lattice symmetry in order to determine which values of J_τ correlate with the lattice rotational levels.

There are a total of $2J+1$ degenerate asymmetric rotator states within each level J_τ, with the eigenfunctions forming an irreducible representation $D^{(J)}$ of the three dimensional rotation group. The decomposition of $D^{(J)}$ with respect to the octahedral point group is thus identical to that of the corresponding Jth spherical harmonic representation, for which the correlations are well known from the theory of atomic crystal field splittings.[10] For $J\leq 5$ the reduction of $D^{(J)}$ is

$$\begin{aligned} &D^{(0)}=A_1, && D^{(1)}=T_1,\\ &D^{(2)}=E+T_2, && D^{(3)}=A_2+T_1+T_2,\\ &D^{(4)}=A_1+E+T_1+T_2, && D^{(5)}=E+2T_1+T_2. \end{aligned} \tag{2.23}$$

Further comparison with the lattice states is possible using the classification of asymmetric rotor levels with respect to C_2^a and C_2^c rotations.[8] Since the highest energy lattice state A_{2u}^+ evidently correlates with $J=3$, we expect that the remaining lattice states also represent exact states having $J\leq 3$.

A compilation of the symmetries and the correspondence of these J_τ levels to the lattice rotation levels appears in Table VI. Also listed are average experimental[11] H_2O energies of the states for comparison with the spectra of T_τ^0 and R^0 calculated using data in Tables IV and V. The energy level orderings of both experiment and theory are identical, although our definition of an experimental average is rather arbitrary. For the higher levels the lattice energies are roughly $\frac{1}{2}$ the experimental averages. This disparity is hardly surprising considering the short wavelength limitations of any

TABLE VI. Exact asymmetric rotor levels J_τ having octahedral symmetry components identical to the discrete hopping model state ($J\leq 3$ only).

Hopping state	Body-fixed symmetry[a]	J_τ values	Average energy (cm^{-1})[b]	lattice energy[c]	
				T_τ^0	R^0
A_{1g}^+	++	0_0	0	0	0
T_{1u}^-	−+	1_{-1}, (3_{-3}, 3_1)[d]	23.8	23.8	34.5
T_{1u}^+	−−	1_0, (3_{-2}, 3_2)[d]	37.1	37.2	
T_{1g}^-	+−	1_1, (3_{-1}, 3_3)[d]	42.4	42.4	
E_u^+	−−	2_0	95.2	47.6	51.7
E_g^+	++	2_{-2}, 2_2	103.1	55.7	
T_{2g}^-	+−	2_{-1}, 3_{-1}	126.4	61.0	68.9
T_{2g}^+	++	2_{-2}, 2_2, 3_0	137.5	66.2	
T_{2u}^-	−+	2_1, 3_{-3}, 3_1	161.3	79.6	
A_{2u}^+	−−	3_{-2}, 3_2	213.7	103.4	103.4

[a] Signs of eigenvalues for body-fixed rotations C_2^a and C_2^c, respectively.
[b] Averaging assumes equal weights for indicated J_τ levels, using experimental H_2O rotation levels of Ref. 11.
[c] Described in Table V.
[d] Not included in energy average.

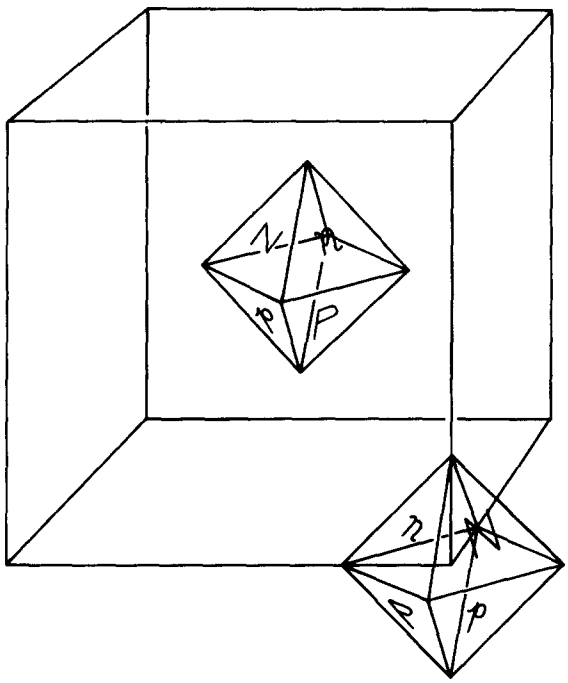

FIG. 2. Geometric representation of the configurations permitted to a pair of neighboring water molecules.

lattice hopping model, and is analogous to errors that appear in the translational spectrum.[5]

III. WATER-MOLECULE INTERACTIONS

The existing papers devoted to lattice-gas models of water employ several different versions of the intermolecular interaction potential V.[1-4] It seems advisable at this stage to reexamine prospects for simple representation of V in the light of current knowledge about water-molecule interactions.

Accurate Hartree–Fock calculations[12-14] have shown that nonadditive components to the interaction in water-molecule aggregates are clearly present. However, these components have modest magnitudes, and vary in sign so as to cancel to some extent. Consequently, we feel justified in assuming at the lattice-gas level of precision that V consists solely of an additive combination of molecular pair interactions

$$V = \sum_{i<j=1}^{N} V^{(2)}(\alpha_i, \omega_i; \alpha_j, \omega_j). \tag{3.1}$$

Formation of linear hydrogen bonds between neighboring molecules is the single most important feature which $V^{(2)}$ must display. In the liquid and solid forms of water, these hydrogen bonds possess lengths in the range 2.75–2.90 Å[15]; consequently the neighbor spacing in the bcc lattice-gas model should likewise fall in this range.

The $(24)^2 = 576$ configurations permitted to a pair of neighboring water molecules may easily be classified according to Fig. 2. In this geometric representation each water molecule is rendered as a regular octahedron with labelled faces. These octahedra must always be oriented so that outward normals to their triangular faces point directly toward the eight nearest-neighbor sites. Pairs of faces are labelled with letters P, p, N, and n. P stands for "proton," and identifies a face out through which an OH bond can be imagined to point. Inversely, N represents the negative regions occupied by (tetrahedrally hybridized) lone pairs of electrons. A well-formed hydrogen bond would require that adjacent P and N faces be presented to one another. Labels p and n identify faces which share two edges, respectively, with P or with N faces.

One easily verifies that the following numbers of configurations exist, totalling 576, for a neighbor pair of water molecules:

$$\begin{aligned}&(PP) = (pp) = (nn) = (NN) = 36,\\ &(Pp) = (Pn) = (PN) = (pn) = (pN) = (nN) = 72.\end{aligned} \tag{3.2}$$

Use of these adjacent-face labels constitutes only a partial classification of nearest-neighbor dimer configurations. Within each such category, C_3 rotations of one of the participating molecules about the line of centers is possible, leading to inequivalent dimer configurations. $V^{(2)}$ would be expected to vary somewhat under these rotations, but that variation would be rather modest since hydrogen bonds would never be formed or broken.

We propose that a qualitatively reasonable lattice-gas $V^{(2)}$ could be constructed in which (a) $V^{(2)}$ is infinite if both molecules reside on the same site, (b) $V^{(2)} = 0$ for all separations beyond the first-neighbor distance, and (c) when molecules are first neighbors $V^{(2)}$ depends only on the labelling of the adjacent octahedron faces shown in Fig. 2. The 10 distinct values of the nearest-neighbor potential, $V^{(2)}(PP)$, $V^{(2)}(Pp)$, $\cdots$, $V^{(2)}(NN)$, should suffice to create tetrahedral hydrogen-bond order for the cubic ice Ic that can fit on the bcc lattice, as well as the partially disordered (but still prejudicially tetrahedral) hydrogen-bond networks that characterize the liquid phase.[16]

We remark in passing that the bcc lattice can in principle accommodate two interpenetrating ice Ic networks. The resulting high-density structure is realized in nature as the high-pressure ices VII and VIII.[15] In order to destabilize these interpenetrating networks at low pressure, Bell invoked a positive three-molecule interaction which acted in compact groupings of those three molecules.[2] However, such nonadditive interactions are not obligatory in the present view (and are not indicated by Hartree–Fock studies); pairs of neighboring molecules with one in each of the two unconnected networks will experience interactions $V^{(2)}(pp)$, $V^{(2)}(pn)$, or $V^{(2)}(nn)$ only. Provided that these quantities are sufficiently high in energy, the requisite destabilization will automatically occur.

No doubt interactions are important between water molecules beyond the first-neighbor distance. These longer-range interactions would predominately be of dipole–dipole form. If the major objective were to study dielectric behavior, it would be necessary to incorporate this extension into the present theory. Our proposed form of nearest-neighbor interaction, how-

TABLE VII. Nearest-neighbor interactions for pairs of water molecules. [a]

Configuration	$V^{(2)}$(kcal/mole)
PP	8.678
Pp	1.662
Pn	−1.762
PN	−5.871
pp	0.948
pn	−0.388
pN	−0.931
nn	1.206
nN	2.156
NN	5.192

[a]The values listed here refer to the octahedron-face categories illustrated in Fig. 2, and were estimated from the "ST2" potential (Ref. 16) at oxygen–oxygen separation 2.85 Å.

ever, enjoys the advantage of great simplicity and should permit application of well-known methods for nearest-neighbor lattice gases in the statistical mechanics.[17] It is our belief that the present nearest-neighbor form for $V^{(2)}$ is a reasonable "zeroth-order" model, into which longer-range dipolar forces could eventually be inserted by standard perturbation theory.

Table VII provides a set of values for the 10 $V^{(2)}$ nearest-neighbor categories. These values were estimated from the semiempirical "ST2" potential that has been reasonably successful in representing liquid water through the molecular dynamics simulation technique.[16]

IV. DIMER VARIATIONAL GROUND STATE ENERGY

The lattice wavefunction for the ground state of the water dimer, having zero center of mass translational motion, may be written in the form

$$\Psi = \Psi^{(1)} + b_2\Psi^{(2)} + b_3\Psi^{(3)} + \cdots, \tag{4.1}$$

where $\Psi^{(n)}$ vanishes except for relative dimer configurations at nth nearest neighbor positions. In general,

$$\Psi^{(n)} = \sum_{\alpha_1}\sum_{\alpha_2}{}' \varphi^{(n)}(\alpha_1, \omega_1; \alpha_2, \omega_2), \tag{4.2}$$

where α_1 runs over all lattice positions for molecule 1, and α_2 includes only the nth nearest-neighbor sites for molecule 2 relative to molecule 1. Furthermore, we can write

$$\varphi^{(n)}(\alpha_1, \omega_1, \alpha_2, \omega_2) = \sum_{\omega_1,\omega_2} |\omega_1, \omega_2\rangle a_n(\alpha_1, \omega_1, \alpha_2, \omega_2), \tag{4.3}$$

where $|\omega_1, \omega_2\rangle$ is a direct-product state vector for the two rotational degrees of freedom, and the a_n are suitable coefficients.

In order to estimate the zero-point energy of the lattice dimer, we have performed a simple variational calculation on the ground state. The trial wavefunction used, Ψ_0, was obtained from Eqs. (4.1)–(4.3) by applying the following constraints:

$$b_n = 0 \qquad \text{if } n > 5, \tag{4.4}$$

$$a_n(\alpha_1, \omega_1, \alpha_2, \omega_2) = 1 \qquad \text{if } n > 1, \tag{4.5}$$

$$a_1(\alpha_1, \omega_1, \alpha_2, \omega_2) = 1 \qquad \text{if the dimer is hydrogen bonded,} \tag{4.6}$$

$$a_1(\alpha_1, \omega_1, \alpha_2, \omega_2) = \eta \qquad \text{if the dimer is not hydrogen bonded.} \tag{4.7}$$

This form permits free monomer rotation for all but nearest-neighbor positions.

The variational energy is obtained by minimizing

$$E_0 = \langle\Psi_0|\mathbf{H}|\Psi_0\rangle / \langle\Psi_0|\Psi_0\rangle \tag{4.8}$$

with respect to b_1, b_2, b_3, b_4, b_5, and η in the limit of an infinitely extended lattice. Evaluation of E_0 reduces to a simple counting procedure over lattice sites, the details of which we shall omit.

For the dimer Hamiltonian H we have used monomer rotational energy operators T^0_r, defined earlier in Eq. (2.20), and the nearest-neighbor pair potential specified in Sec. III and Table VII. The corresponding variational energy expression is

$$E_0 = W/Q, \tag{4.9}$$

with

$$W = \epsilon_0 + \epsilon_1\eta^2 + 12r(1-\eta)^2 - 4t[(1+7\eta)(3b_2+3b_3+b_5) + 24(b_2+2b_3+b_5)b_4] \tag{4.10}$$

and

$$Q = 1 + 7\eta^2 + 6b_2^2 + 12b_3^2 + 24b_4^2 + 8b_5^2. \tag{4.11}$$

Here we have employed the definitions

$$t = \hbar^2/2ml^2, \qquad r = (A+B+C)/6, \qquad \epsilon_0 = V^{(2)}(N,P),$$
$$\epsilon_1 = V^{(2)}(pn) + V^{(2)}(pN) + V^{(2)}(pP) + V^{(2)}(nN) + V^{(2)}(nP) + \tfrac{1}{2}[V^{(2)}(nn) + V^{(2)}(pp) + V^{(2)}(PP) + V^{(2)}(NN)]. \tag{4.12}$$

An identical expression for E_0, and in particular for the rotational energy contribution $12r(1-\eta)^2$ in Eq. (4.10), is obtained using the simpler R^0 form for monomer rotation energy [Eqs. (2.21)–(2.22)]. At the present level of approximation this result must be regarded as somewhat fortuitous.

Using $l = 2.85$ Å, and information contained in Table IV for rotational parameters, and in Table VII for interactions, the variational energy E_0 has been minimized for each of $H_2{}^{16}O$, $D_2{}^{16}O$, and $T_2{}^{16}O$. The numerical results are contained in Table VIII. Although

TABLE VIII. Results of variational calculations for the ground state of the lattice water dimer. [a]

	$H_2{}^{16}O$	$D_2{}^{16}O$	$T_2{}^{16}O$
E	−5.5772	−5.7140	−5.7599
$E-V^{(2)}(PN)$	0.2938	0.1570	0.1111
η	0.00615	0.00322	0.00226
$10^5 b_2$	6	5	5
$10^5 b_3$	3	3	2
b_4	0	0	0
$10^5 b_5$	2	1	1

[a]Energies in kcal/mole.

the zero-point energy destabilization of the hydrogen bond,

$$\Delta E = E_0(\min) - V^{(2)}, \tag{4.13}$$

is significant in each case, it is obvious from the values of $\eta \cdots b_5$ that rather little tunneling out of the bonded configurations is involved. Probably our assumptions (4.4)–(4.7) that Ψ is independent of relative orientation (if no bond is present) tends somewhat to retard that tunneling. In any event, the magnitudes obtained for ΔE seem roughly to be consistent with thermodynamic property differences between the three isotopic waters.[15]

It should be pointed out that real water dimers may exhibit isotope shifts in their binding energies due to changes in vibrational zero-point energy when the free molecules form a hydrogen bond. However, this will entail partially cancelling effects, since the OH bond stretch should experience a force constant reduction on bonding, while the bend mode should be stiffened. It will be desirable eventually to include these internal degrees of freedom in a more complete theoretical study of binding in the dimer.

V. QUANTUM CORRECTIONS IN THE STATISTICAL THEORY

A. Definitions

We now consider the thermal equilibrium behavior of N water molecules on the bcc lattice. The N-molecule Hamiltonian operator

$$\mathrm{H} = \mathrm{T} + \mathrm{V} \tag{5.1}$$

consists of the kinetic and potential energy operators specified in Eqs. (1.1) and (3.1), respectively. The corresponding partition function Z and associated free energy F at absolute temperature T are given by

$$Z = \mathrm{Tr}[\exp(-\beta \mathrm{H})] \equiv \exp(-\beta F), \qquad \beta = (k_B T)^{-1}, \tag{5.2}$$

where the trace involves a basis suitable for the given isotopic species.

Let the eigenvalues of H be denoted by E_μ. Since the lattice-gas model confines the separate molecules to a discrete set of positions and orientations, there will be a finite number M of eigenvalues (provided the lattice is finite) so we take $1 \le \mu \le M$. Thus, we can write

$$\beta F = -\ln\left[\sum_{\mu=1}^{M} \exp(-\beta E_\mu)\right] = -\ln M - \ln\langle \exp(-\beta E_\mu)\rangle, \tag{5.3}$$

where the angular brackets denote an unweighted average over eigenvalues,

$$\langle f(E_\mu)\rangle = \frac{1}{M}\sum_{\mu=1}^{M} f(E_\mu). \tag{5.4}$$

Equation (5.3) may be expanded in a β power series, with coefficients that are cumulants of spectral moments[18]:

$$\beta F = -\ln M + \beta\langle E_\mu\rangle - \tfrac{1}{2}\beta^2[\langle E_\mu^2\rangle - \langle E_\mu\rangle^2] + \tfrac{1}{6}\beta^3[\langle E_\mu^3\rangle - 3\langle E_\mu^2\rangle\langle E_\mu\rangle + 2\langle E_\mu\rangle^3] - \cdots. \tag{5.5}$$

The "classical limit" partition function Z_0 corresponds to the limit in which the molecular mass and moments of inertia all become infinite. This limit causes the kinetic energy operator T to vanish, so that the E_μ are then eigenfunctions of V alone.

Molecular distribution functions $P^{(s)}$ may be defined as follows:

$$P^{(s)}(\alpha_1, \omega_1, \cdots, \alpha_s, \omega_s) = Z^{-1}\,\mathrm{Tr}\left[\exp(-\beta \mathrm{H})\prod_{j=1}^{s} \mathrm{n}(\alpha_j, \omega_j)\right], \tag{5.6}$$

where $\mathrm{n}(\alpha, \omega)$ is the number operator for molecules on site α with orientation ω. $P^{(s)}$ gives the probability that the given s sites are simultaneously occupied with the specified orientations. The "classical limit" distribution functions $P_0^{(s)}$ naturally correspond to setting T = 0 in both numerator and denominator of Eq. (5.6).

B. Low density limit

If the number of sites Ω in the bcc lattice far exceeds the number of molecules N, the system will comprise a dilute vapor in which collisions are rare. Then provided the temperature is not too low (to avoid clustering), the molecules will virtually always be free and will move independently. The N-molecule energy spectrum may then be regarded as composed additively of single-molecule energies ϵ_ν, where $1 \le \nu \le M_1$. Taking due account of molecule identity, we have in this case

$$M = (M_1)^N/N!\,. \tag{5.7}$$

Consequently, in the dilute vapor regime the N-molecule partition function Z may be expressed simply in terms of the single-molecule partition function Z_1:

$$Z \cong \frac{(Z_1)^N}{N!}, \quad Z_1 = \sum_{\nu=1}^{M_1} \exp(-\beta\epsilon_\nu). \tag{5.8}$$

Just as it was possible to generate the cumulant expansion (5.5) for the full N-molecule spectrum, so can a similar cumulant expansion be generated for the single-molecule spectrum. In this way we can verify that the low-density form for Eq. (5.5) is as follows:

$$\beta F = N\{-\ln(eM_1/N) + \beta\langle\epsilon_\nu\rangle_1 - \tfrac{1}{2}\beta^2[\langle\epsilon_\nu^2\rangle_1 - \langle\epsilon_\nu\rangle_1^2] + \tfrac{1}{6}\beta^3[\langle\epsilon_\nu^3\rangle_1 - 3\langle\epsilon_\nu^2\rangle_1\langle\epsilon_\nu\rangle_1 + 2\langle\epsilon_\nu\rangle_1^3] - \cdots\}, \tag{5.9}$$

where now

$$\langle f(\epsilon_\nu)\rangle_1 = \frac{1}{M_1}\sum_{\nu=1}^{M_1} f(\epsilon_\nu). \tag{5.10}$$

The obvious isomorphism of cumulants in Eqs. (5.5) and (5.9) persists to all orders on account of the fact that E_α is additively composed of N independently distributed variables ϵ_ν.[18]

Since we have assumed from the outset that translational and rotational motion do not couple, each ϵ_ν will itself consist of separate translational (t) and rotational (r) parts:

$$\epsilon_\nu = \epsilon_t + \epsilon_r. \tag{5.11}$$

This permits the cumulant series (5.9) once again to be resolved into separate components for the individual

degrees of freedom:

$$\beta F/N = -\ln(eM_1/N) + \beta\{\langle\epsilon_t\rangle_1 + \langle\epsilon_r\rangle_1\} - \tfrac{1}{2}\beta^2\{[\langle\epsilon_t^2\rangle_1 - \langle\epsilon_t\rangle_1^2] + [\langle\epsilon_r^2\rangle_1 - \langle\epsilon_r\rangle_1^2]\} + \tfrac{1}{6}\beta^3\{[\langle\epsilon_t^3\rangle_1 - 3\langle\epsilon_t^2\rangle_1\langle\epsilon_t\rangle_1 + 2\langle\epsilon_t\rangle_1^3] + [\langle\epsilon_r^3\rangle_1 - 3\langle\epsilon_r^2\rangle_1\langle\epsilon_r\rangle + 2\langle\epsilon_r\rangle^3]\} - \cdots . \quad (5.12)$$

The translational energies, for periodic boundary conditions, are easily found to be

$$\epsilon_t(\mathbf{k}) = (4\hbar^2/ml^2)[1 - \cos(\tfrac{1}{2}k_x l)\cos(\tfrac{1}{2}k_y l)\cos(\tfrac{1}{2}k_z l)], \quad (5.13)$$

where the Ω vectors $[\mathbf{k} = (k_x, k_y, k_z)]$ form the dodecahedral first Brillouin zone for the bcc lattice.[19] Notice that near $\mathbf{k} = 0$ the dispersion relation (5.13) is locally parabolic, and agrees with that for translation in free space.

Rotational energies ϵ_r were determined in Sec. II above, and may be extracted from Tables IV–VI. It is important to recall that the levels listed there may be either even (+) or odd (−) under hydrogen atom exchange, so care must be exercised to select the correct weights depending on hydrogen isotope nuclear spins $S(=\frac{1}{2}, 1, \text{and } \frac{1}{2}$, for H, D, and T, respectively).

In the classical limit defined above, all single-molecule energies (both translational and rotational) collapse identically to zero. Each cumulant in series (5.12) likewise vanishes in the classical limit. By restoring $\mathbf{T}$ to the problem the energy levels are shifted and spread apart, so as to produce nonvanishing cumulants in Eq. (5.12).

Using energy units β^{-1}, the shift expected for translational energies ϵ_t will be proportional to the dimensionless parameter[5]

$$X = \beta\hbar^2/2ml^2. \quad (5.14)$$

The analogous dimensionless quantity for rotational energy shifts may be taken to be

$$Y = \beta(A + B + C)/6. \quad (5.15)$$

The free energy series (5.12) for the dilute vapor could be written as separate power series in X and Y with no cross terms. Since collisions can produce coupling between translation and rotation, we expect cross terms in X and Y to occur at higher vapor density, and to be significant in liquid and solid phases of water.

In the case of $H_2{}^{16}O$ at 0 °C, X and Y have the following values (assuming that the nearest-neighbor distance is 2.85 Å):

$$X = 6.069\times10^{-4}, \quad Y = 4.537\times10^{-2}. \quad (5.16)$$

The relative importance of these parameters cannot be judged before examining their respective coefficients in the series of interest.

C. Asymptotic free energy corrections

We now examine the case of arbitrary density. With respect to the free energy F, we seek explicit expressions for corrections to the classical-limit free energy F_0 in leading orders of X and Y. For this purpose it is convenient to use the following formal expansion[5,20]:

$$\exp(-\beta\mathbf{H}) = \mathbf{G}_0(1) - \beta\int_0^1 d\lambda_1\,\mathbf{G}_0(\lambda_1)\,\mathbf{T}\mathbf{G}_0(1-\lambda_1) + \cdots + (-\beta)^n\int_0^1 d\lambda_1\int_0^{1-\lambda_1} d\lambda_2\cdots\int_0^{1-\lambda_1-\cdots-\lambda_{n-1}} \mathbf{G}_0(\lambda_1)\mathbf{T}\mathbf{G}_0(\lambda_2)\,\mathbf{T}\cdots\mathbf{G}_0(\lambda_n)\,\mathbf{T}\mathbf{G}_0(1-\lambda_1-\cdots-\lambda_n) + \cdots . \quad (5.17)$$

Here we have written

$$\mathbf{G}_0(\lambda) = \exp(-\lambda\beta\mathbf{V}). \quad (5.18)$$

In order to keep the discussion as simple as possible, we shall use the spherical rotor form (2.21) for the rotational kinetic energy operator. Referring as well to Eq. (1.2), one has

$$\beta\mathbf{T} = X\mathcal{T}_t + Y\mathcal{T}_r, \quad (5.19)$$

where X and Y have been defined above [in Eqs. (5.14) and (5.15)], and operators $\mathcal{T}_t$ and $\mathcal{T}_r$ are devoid of physical parameters (β, m, $\hbar$, l, A, B, C). In particular these operators have the following properties when operating on the N-molecule wavefunction Ψ:

$$\mathcal{T}_t\,\Psi(\alpha,\omega) = 8N\Psi(\alpha,\omega) - \sum_{\alpha'}\Psi(\alpha',\omega),$$
$$\mathcal{T}_r\,\Psi(\alpha,\omega) = 6N\Psi(\alpha,\omega) - \sum_{\omega'}\Psi(\alpha,\omega'). \quad (5.20)$$

Here α comprises the full set of occupied sites with only single occupancy permitted; the sets α' included in the summation differ from α in that one molecule has been displaced (with fixed orientation) to an empty nearest-neighbor site. Likewise ω comprises all N molecular orientations; the permissible ω' differ only by a single C_4 rotation of any of the molecules.

When expressions (5.19) and (5.20) are used to replace $\beta\mathbf{T}$ in Eq. (5.17), the resulting operator series can be used to calculate the trace required by partition function Z in Eq. (5.2). It is clear that terms of all orders in X and Y will be generated by that procedure including cross terms. We omit details since they parallel those in Ref. 5 so closely. The final result will have the following form:

$$\ln Z = \ln Z_0 + \sum_{\substack{l,n=1\\(l+n>0)}}^{\infty}\Lambda_{l,n}(\beta)X^l Y^n, \quad (5.21)$$

where of course

$$Z_0 = \mathrm{Tr}[\exp(-\beta\mathbf{V})]$$

provides the classical-limit partition function.

The leading coefficients $\Lambda_{1,0}$ and $\Lambda_{0,1}$ involve only the diagonal parts of the operators $\mathcal{T}_t$ and $\mathcal{T}_r$. Consequently, they are trivial to evaluate. One finds

$$\Lambda_{1,0} = -8N, \quad \Lambda_{0,1} = -6N. \tag{5.22}$$

Since the corresponding contribution to the free energy F, namely $-N(8X+6Y)/\beta$, is independent both of temperature and volume, these leading-order quantum corrections cannot affect the pressure equation of state [recall that $p = -(\partial F/\partial V)_{N,T}$].

The second-order corrections in Eq. (5.21) involve the nondiagonal parts of $\mathcal{T}_t$ and $\mathcal{T}_r$. In particular, two molecular shifts (in position or orientation) must occur, after which the system of molecules has returned either to its original configuration or to one equivalent to it by permutation of identical particles (with identical spin variables). This requirement can be satisfied in three ways:

(a) shift of any one of the N molecules (at fixed orientation) to an empty nearest-neighbor site, and then back again;

(b) C_4 rotation of any molecule, followed by the inverse rotation to restore the original configuration;

(c) two successive rotations C_4^b (in the same sense) so as to interchange positions of hydrogen nuclei with identical spin variables.

The first of these provides coefficient $\Lambda_{2,0}$, while the second and third combine to give $\Lambda_{0,2}$. Since the given requirement cannot be satisfied with one translational shift and one rotational shift, $\Lambda_{1,1}$ must vanish.

In order to give explicit form to the second-order quantum corrections, it is necessary to introduce a "shift probability" Q_0 for the classical-limit lattice gas. Specifically, the symbol $Q_0(\alpha, \omega; \alpha', \omega'; \Delta V)$ will stand for the probability (in the classical limit) that (1) site α is occupied by a molecule with orientation ω, (2) site α' (if it is distinct from α) is empty, and (3) that transfer of the molecule at α, ω to α', ω' causes the total potential energy to change by ΔV.

With this definition in hand, one obtains

$$\Lambda_{2,0} = \sum_{\substack{\alpha,\alpha',\omega,\omega' \\ \Delta V}} Q_0(\alpha, \omega; \alpha', \omega'; \Delta V)\, f(\beta \Delta V), \tag{5.23}$$

where

$$f(x) = \frac{1}{x}\left[1 + \frac{\exp(-x) - 1}{x}\right] \tag{5.24}$$

is a monotonically decreasing positive function of x. In the summations indicated in Eq. (5.23), α covers all lattice sites, but α' is restricted to be a nearest neighbor of α. With potential energy V restricted to the form discussed in Sec. III, ΔV can have only a finite set of distinct values, all of which must be included in the summation. Similarly, one finds

$$\Lambda_{0,2} = \sum_{\alpha,\omega,\Delta V}\left[\sum_{\omega'}^{(C_4)} Q_0(\alpha, \omega; \alpha, \omega'; \Delta V) f(\beta \Delta V) \pm (2S+1)^{-1} \sum_{\omega'}^{(C_4^b)} Q_0(\alpha, \omega; \alpha, \omega'; \Delta V) f(\beta \Delta V)\right], \tag{5.25}$$

where S stands for the hydrogen-isotope nuclear spin. The first ω' summation [corresponding to (b) above], includes all C_4 rotations from ω, while the second includes only those about the molecular symmetry axis. The upper sign is appropriate for bosons (i.e., deuterons), the lower for fermions (protons or tritons).

In contrast to the first-order corrections, the second-order contributions affect the pressure equation of state. Since $\Lambda_{2,0}$ is always positive it acts to reduce F; however, its ability to do so is hampered at high compression due to lack of empty sites into which translational shifts could occur. Consequently, lower densities receive greater $\Lambda_{2,0}$ stabilization, and in particular this term will act to raise the vapor pressure of condensed phases. Similar comments apply to the first part of $\Lambda_{0,2}$ in Eq. (5.25), corresponding to category (b) of C_4 rotations and returns. The exchange part of $\Lambda_{0,2}$, corresponding to category (c) with two C_4^b rotations, acts in the same way for bosons (D) but oppositely for fermions (H, T).

Following the procedure outlined in Ref. 5, higher-order quantum corrections for F can also be derived. They require knowledge of n-step shift probabilities (including both translations and rotations) in the classical-limit ensemble. The results are rather complicated, and we do not reproduce them here. We remark only that with the bcc lattice, cross terms involving both X and Y are encountered first in fourth order, where $\Lambda_{2,2} \neq 0$.

D. Molecular distribution functions

For completeness, we now state the leading-order quantum corrections for the molecular distribution functions $P^{(s)}$ that were defined in Eq. (5.6). Except for minor modifications the derivations follow those provided in Ref. 5 and again rely on the operator expansion (5.17).

No first-order corrections arise for any $P^{(s)}$. In order to express the second-order corrections, it is necessary to introduce a generalization of Q_0 above, to accommodate the site occupancy required by $P^{(s)}$. Let

$$Q_0^{(s)}(\bar{\alpha}_1, \bar{\omega}_1, \cdots, \bar{\alpha}_s, \bar{\omega}_s \mid \alpha, \omega; \alpha', \omega'; \Delta V) \tag{5.26}$$

represent the classical-limit probability that (1) initially sites $\bar{\alpha}_1 \cdots \bar{\alpha}_s$ are occupied by molecules with respective orientations $\bar{\omega}_1 \cdots \bar{\omega}_s$, (2) site α (possibly one of $\bar{\alpha}_1 \cdots \bar{\alpha}_s$) initially has a molecule with orientation ω, (3) site α' is initially empty, and (4) shift of the particle from α, ω to α', ω' causes the total potential to change by amount ΔV. At least in the fluid region of the phase diagram, $Q_0^{(s)}$ should reduce to the prior Q_0 if α and α' are widely separated from $\bar{\alpha}_1 \cdots \bar{\alpha}_s$.

One finds

$$P^{(s)}(\bar{\alpha}_1 \cdots \bar{\omega}_s) = P_0^{(s)}(\bar{\alpha}_1 \cdots \bar{\omega}_s)\,[1 + \Lambda_{2,0}^{(s)}(\bar{\alpha}_1 \cdots \bar{\omega}_s)\,X^2 + \Lambda_{0,2}^{(s)}(\bar{\alpha}_1 \cdots \bar{\omega}_s)\,Y^2 + \cdots], \tag{5.27}$$

where

$$\Lambda_{2,0}^{(s)} = \sum_{\substack{\alpha,\alpha',\omega, \\ \Delta V}} f(\beta \Delta V)\,[Q_0^{(s)}(\bar{\alpha}_1 \cdots \bar{\omega}_s |\, \alpha, \omega; \alpha', \omega; \Delta V) - Q_0(\alpha, \omega; \alpha', \omega; \Delta V)] \tag{5.28}$$

and

$$\Lambda_{0,2}^{(s)} = \sum_{\alpha,\omega,\Delta V} \Bigg\{ \sum_{\omega'}^{(C_4)} [Q_0^{(s)}(\bar{\alpha}_1 \cdots \bar{\omega}_s |\, \alpha, \omega; \alpha, \omega'; \Delta V) - Q_0(\alpha, \omega; \alpha, \omega'; \Delta V)]\, f(\beta \Delta V)$$

$$\pm (2S+1)^{-1} \sum_{\omega'}^{(C_4^b)} [Q_0^{(s)}(\bar{\alpha}_1 \cdots \bar{\omega}_s |\, \alpha, \omega; \alpha, \omega'; \Delta V) - Q_0(\alpha, \omega; \alpha, \omega'; \Delta V)]\, f(\beta \Delta V) \Bigg\} \,. \tag{5.29}$$

The function f was defined in Eq. (5.24). The same summation conventions apply in Eqs. (5.28) and (5.29) that did for the analogous Eqs. (5.23) and (5.25).

The results shown for $\Lambda_{2,0}^{(s)}$ and $\Lambda_{0,2}^{(s)}$ have an obvious interpretation. The presence of s particles in $\bar{\alpha}_1 \cdots \bar{\omega}_s$ influences the second-order free energy corrections involving two-step translational or rotational shifts. The relative degree to which these fixed particles stabilize or destabilize the system influences the probability of their spontaneous occurrence in the canonical ensemble, and $P^{(s)}$ is affected accordingly.

VI. DISCUSSION

All of the calculations in the present paper have been based on the body-centered cubic lattice illustrated in Fig. 1. The sites in this lattice afford only a coarse subdivision of space, so that it is desirable to identify finer lattices for future applications.

With respect to translational motion, it has been pointed out before[21] that the bcc lattice can be embedded in a fcc array with 16 times the site density. Sites which were originally nearest neighbors become sixth-neighbors. Use of this higher density array would permit hydrogen-bond bending, stretching, and compression to occur, as it surely must in real liquid water. Hydrogen-bond polygons with an odd number of sides become possible for the first time.

In principle this increase in density of translational sites could be implemented while retaining the same 24 discrete orientations permitted at the outset. However, it seems at least as important to provide a larger number of orientations.

Figure 3 shows that a regular pentagonal dodecahedron can be erected about a cube, such that the vertices of the latter are coincident with eight of the 20 vertices of the former. If a water molecule is located at the center of the cube, it has 120 distinct orientations (regarding its hydrogens as distinguishable) that point OH groups toward pairs of pentagonal vertices. Of course one-fifth of these are the original 24 orientations for the cube alone.

Examination of Fig. 3 shows that there are two ways that the dodecahedron can be placed around the cube. Using both ways simultaneously to define acceptable orientations leads to a total of 216 molecular orientations, nine times as many as permitted in the elementary bcc model. No doubt this elaboration would dramatically improve ability to fit the lower portion of the water-molecule rotational spectrum.

All lattice-gas models for water to date have treated the individual molecules as rigid and forever stable. However, it should be noted that this point of view can be relaxed to allow molecular dissociation into H^+ and OH^-. The most straightforward way to achieve this end is to treat the entire collection of O and H nuclei as dynamically distinct entities subject to a suitable set of forces which can cause molecules spontaneously to form; in fact these forces can be central and additive.[22] The bcc lattice would still be a suitable set of sites for oxygens, while trisection of each O–O nearest-neighbor line would provide suitable sites for hydrogens.

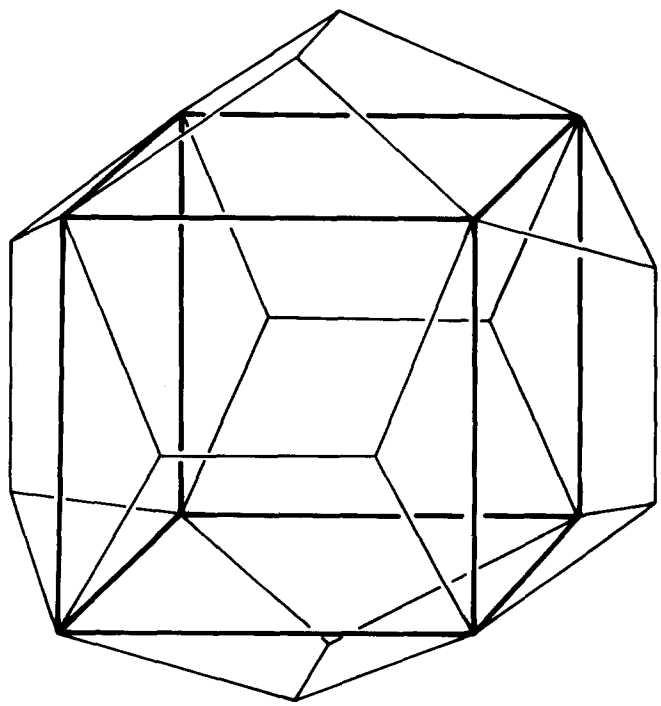

FIG. 3. A regular pentagonal dodecahedron erected about a cube, the vertices of the latter being coincident with eight of the 20 vertices of the former.

The resulting theory would provide valuable insights into both equilibrium and kinetic aspects of the dissociation–association process in water.

*Present address: Chemistry Department, University of Oregon, Eugene, OR 97403.

[1]S. Levine and J. W. Perram, in *Hydrogen-Bonded Solvent Systems*, edited by A. K. Covington and P. Jones (Taylor and Francis, London, 1968), pp. 115–129.
[2]G. M. Bell, J. Phys. C 5, 889 (1972).
[3]P. D. Fleming, III and J. H. Gibbs, J. Stat. Phys. **10**, 157 (1974).
[4]P. D. Fleming, III and J. H. Gibbs, J. Stat. Phys. **10**, 351 (1974).
[5]F. H. Stillinger, J. Stat. Phys. (to be published).
[6]W. S. Benedict, N. Gailar, and E. K. Plyler, J. Chem. Phys. **24**, 1139 (1956).
[7]See, for instance, M. Tinkham, *Group Theory and Quantum Mechanics* (McGraw-Hill, New York, 1964), Chaps. 3–4.
[8]For a description of the asymmetric rotor and the labelling conventions of the energy levels, see G. Herzberg, *Infrared and Raman Spectra of Polyatomic Molecules* (Van Nostrand Reinhold, New York, 1945), pp. 42–55.
[9]J. Bellet, G. Steenbeckeliers, and P. Stouffs, C. R. Acad. Sci. Ser. B **275**, 501 (1972).
[10]H. Bethe, Ann. Phys. Leipzig **3**, 133 (1929).
[11]R. T. Hall and J. M. Dowling, J. Chem. Phys. **47**, 2454 (1967).
[12]D. Hankins, J. W. Moskowitz, and F. H. Stillinger, J. Chem. Phys. **53**, 4544 (1970); erratum: J. Chem. Phys. **59**, 995 (1973).
[13]B. R. Lentz and H. A. Scheraga, J. Chem. Phys. **58**, 5296 (1973).
[14]H. Kistenmacher, G. C. Lie, H. Popkie, and E. Clementi, J. Chem. Phys. **61**, 546 (1974).
[15]D. Eisenberg and W. Kauzmann, *The Structure and Properties of Water* (Oxford University, New York, 1969).
[16]F. H. Stillinger and A. Rahman, J. Chem. Phys. **60**, 1545 (1974).
[17]C. Domb, Adv. Phys. **9**, 245 (1960).
[18]H. Cramér, *Mathematical Methods of Statistics* (Princeton University, Princeton, 1946), Chap. 15.
[19]L. Brillouin, *Wave Propagation in Periodic Structures* (Dover, New York, 1953), 2nd edition, p. 153.
[20]R. P. Feynman, *Statistical Mechanics* (Benjamin, Reading, MA, 1972), p. 67.
[21]F. H. Stillinger, Adv. Chem. Phys. **31**, 1 (1975).
[22]H. L. Lemberg and F. H. Stillinger, J. Chem. Phys. **62**, 1677 (1975).